Design and Full-Scale Implementation of the Largest Operational Electrically Conductive Concrete Heated Pavement System

Amir Malakooti*
Ph.D. Student
24 Town Engineering Building, Department of Civil, Construction and Environmental Engineering (CCEE), Iowa State University, Ames, IA 50011-1066
Phone: +1-801-318-1451
E-mail: amir@iastate.edu
orcid.org/0000-0001-8177-3571

Wei Shen Theh
Ph.D. Student
2215 Coover Hall, Department of Electrical and Computer Engineering (ECpE)
Iowa State University,
Ames, IA 50011-1046
E-mail: wstheh@iastate.edu

S.M. Sajed Sadati
Ph.D. Candidate
403 Town Engineering Building, CCEE
Iowa State University,
Ames, IA 50011-1066
E-mail: ssadati@iastate.edu
orcid.org/0000-0002-5512-5615

Halil Ceylan, Ph.D.
Professor of CCEE
ISU Site Director, FAA PEGASAS (Partnership to Enhance General Aviation Safety, Accessibility and Sustainability) Center of Excellence (COE) on General Aviation
Director, Program for Sustainable Pavement Engineering and Research (PROSPER)
410 Town Engineering Building, CCEE, Iowa State University, Ames, IA 50011-1066
Phone: +1-515-294-8051
E-mail: hceylan@iastate.edu
orcid.org/0000-0003-1133-0366

Sunghwan Kim, Ph.D., P.E.
Research Scientist, Institute for Transportation,
24 Town Engineering Building, CCEE
Iowa State University, Ames, IA 50011-1066
E-mail: sunghwan@iastate.edu
orcid.org/0000-0002-1239-2350

Mani Mina, Ph.D.
Associate Professor of ECpE
341 Durham Center, ECpE
Iowa State University,
Ames, IA 50011-2100
Email: mmina@iastate.edu
orcid.org/0000-0002-1500-9492

Kristen Cetin, Ph.D., P.E.
Assistant Professor of Civil & Environmental Engineering,
474 S. Shaw Lane,
Michigan State University,
East Lansing, MI 48824
E-mail: cetinkri@msu.edu
orcid.org/0000-0003-2662-8480

Peter C. Taylor, Ph.D., P.E.
Director of National Concrete Pavement Technology Center, 2711 S Loop Dr,
Ames, IA 50010-8664
E-mail: ptaylor@iastate.edu
https://orcid.org/0000-0002-4030-1727

*: Corresponding Author

ABSTRACT

Many aviation and transportation agencies allocate significant time and resources each year to remove ice and snow from their paved surfaces to achieve a safe, accessible, and operational transportation network. An electrically conductive concrete (ECON) heated pavement system (HPS) has been shown to be a promising alternative to the conventional snow removal operations using snowplows and deicing chemicals, which is time-consuming, labor-intensive and environmentally unfriendly. ECON HPS utilizes the inherent electrical resistance of concrete to maintain the pavement surface above freezing and thus prevent snow and ice accumulation on the surface. This sustainable concrete pavement system improves the resiliency of infrastructure by allowing it to be safe, open, and accessible during even harsh winter storms. The purpose of this study was to demonstrate the full-scale implementation of 10 ECON HPS slabs at the Iowa Department of Transportation headquarter south parking lot in Ames, Iowa. This study consists of system design and control, field implementation, and sensor instrumentation procedures for the construction of the ECON system, which took place on October 2018. A programmable logic controller (PLC) was designed, programmed, and utilized to control, operate, and monitor the system remotely. The heating performance of the remotely-operated ECON slabs was evaluated using the instrumented sensors under snow and ice events in 2019. The performance evaluation showed promising results in providing snow, and ice-free pavement surfaces through several winter weather events.

Keywords: electrically conductive concrete, heated pavement system, construction, electrode, resistive heating, winter maintenance, Concrete pavement system, Sustainability, Resiliency

1. INTRODUCTION

Removal of snow and ice is an inescapable activity for transportation infrastructure owners in cold climates, to ensure safe and accessible transportation systems. To enhance the capability and resiliency of transportation systems to overcome the challenges that arise during snow events, an electrically conductive concrete (ECON) heated pavement system (HPS) has been developed (*1–4*). This is a special type of heated pavement system (*5–8*) that includes a top concrete layer made by adding electrically conductive material, such as carbon fibers (*9–11*) and steel shavings (*3*) to the concrete mixture (*12*). These systems not only enhance the accessibility of transportation infrastructure but also prevent the excessive need for chemicals and fossil fuel-based vehicles for snow and ice removal. Moreover, ECON HPS is an electricity-based system, and its utilization can help with the ongoing efforts for electrification of processes at airports (*13*), which are more environmentally friendly and can reduce water and air pollution at airports (*2*, *14*).

Weather conditions impact the performance of ECON HPS; therefore, each specific region needs a particular design for ensuring the best performance of the system (*2*). The design parameters for ECON HPS include the thickness of the regular and conductive concrete layers, joint spacing, electrode spacing, and electrode size and shape. Among these parameters, electrode spacing and electrode size and shape are the ones that are unique to the ECON HPS design and are not required for conventional rigid pavement systems. Therefore, the motivation for this study was to investigate the impact of these two parameters on the thermal and energy performance of ECON HPS through a field experimental study. Previous experimental studies on ECON HPS have only focused on investigating the construction and performance, assuming only one design configuration (*3*, *15*).

Abdualla, et al. (*15*), designed ECON HPS test slabs for the general aviation section of Des Moines International Airport (DSM) in Iowa. The ECON was made by adding carbon fibers to the concrete mix, and the design included angled stainless-steel electrodes at a spacing of 91 cm (3 ft). Abdualla found that ECON HPS has the potential to reduce temperature gradient within the pavement thicknesses and consequently reduce the curling stresses (*16*). Tuan (*3*) designed and tested an ECON HPS with vertically positioned steel plates as electrodes having a spacing of 122 cm (4 ft). The ECON material was made by adding steel shavings to the concrete mix, and this setup was tested on a bridge deck in Lincoln, Nebraska, which is out of service since 2009. Use of steel shavings as the conductive material for ECON is not recommended for transportation infrastructure since the steel shavings can potentially corrode and also cause damage to the vehicle tires and aircraft engines by creating foreign object debris (*1*). There are a few other studies on the performance of ECON HPS through numerical models developed using the results of experimental studies (*2*, *17–19*). Only one study previously published with ECON HPS has focused on the performance of this system with various electrode design configurations, which was based on only numerical study and not full-scale experimental study in different real weather condition (*18*).

The objective of the current study was to construct and demonstrate a full-scale implementation procedure of the largest operational ECON HPS with different electrode configurations. Ten full-

scale slabs were constructed at the south parking lot entrance of the Iowa Department of Transportation Headquarter (Iowa DOT) in Ames, Iowa as part of a reconstruction project. These slabs have various configurations of electrodes with different spacing, sizes, and shapes (configuration) in order to evaluate their effect on the energy and thermal performance of the ECON HPS. Other than the 10 ECON HPS slabs, the test setup included two regular concrete slabs as the control sections to compare the structural performance of the ECON HPS to regular rigid pavement systems for future studies. The remainder of this paper provides the implementation overview, description of the materials, instrumentation and installation methods, construction procedures, and slabs performance evaluation during different snow events.

2. FULL-SCALE ECON HPS IMPLEMENTATION OVERVIEW

The test site was located at the south parking lot entrance of Iowa DOT in Ames, Iowa (Figure 1(a)). As part of the reconstruction project, 10 slabs, 4.6 m (15 ft.) long and 3.6 m (12 ft.) wide, were dedicated to the ECON HPS implementation. The slabs close to the south entrance were chosen as the heated pavement test site specifically because it was located in a high and heavy volume of traffic section.

2.1 Key Components of ECON HPS Technology

The key components of ECON HPS technology include an ECON layer (heating element), electrodes, temperature sensors, electrical wiring, polyvinyl chloride (PVC) conduits, control system, and power supply. This technology can be either constructed as an overlay on top of an existing pavement system if the pavement is in good condition, or as a top layer of a two-lift paving for a new construction. Two-lift paving can be used to reduce construction material costs by reducing the ECON layer thickness since it is necessary to heat only the surface of pavement where the snow and ice accumulation occurs. Temperature sensors are installed to give the control system the ability to monitor the pavement surface temperature and set surface temperature to above-freezing temperature (5°C/41°F). This helps to reduce the possibility of overheating and to reduce energy consumption by not continuously operating the system when the surface temperatures are sufficiently warm. The energy consumption due to the thermal performance of ECON HPS can be monitored with wireless voltage and current sensors remotely.

2.2 ECON HPS System Design

The ECON system design consists of procedures to determine the required layer thicknesses for structural adequacy, electrode configuration based on the environmental conditions, and power demand estimation. The layer thicknesses for the Iowa DOT ECON HPS project were designed based on heavy traffic volume. Figure 1(b) is the plan view of the construction site, which shows the 10 slabs, location of conduits, shed, and power supply. All the electrical wiring from the electrodes to the power supply and the sensor wiring in each test section went through trenches to the shed. The control system and the data acquisition system were placed in the shed. Figure 1(c) illustrates the cross-sectional view of different structural layers, which include 22.9 cm (9 in.) special backfill base layer, 17.8 cm (7 in.) C-3WR-C20 regular portland cement concrete (PCC) layer specified in Iowa DOT standard specification, which is explained in detail in section 3.1 (*20*), and a 7.6 cm (3 in.) ECON layer. The electrodes were placed on top of the PCC layer, ensuring a 5 cm (2 in.) concrete cover on top of the electrodes. Special backfill materials that were used for the base layer consisted of crushed stone, crushed PCC, and crushed composite pavement aggregates according to Iowa DOT specification (*20*).

(a)

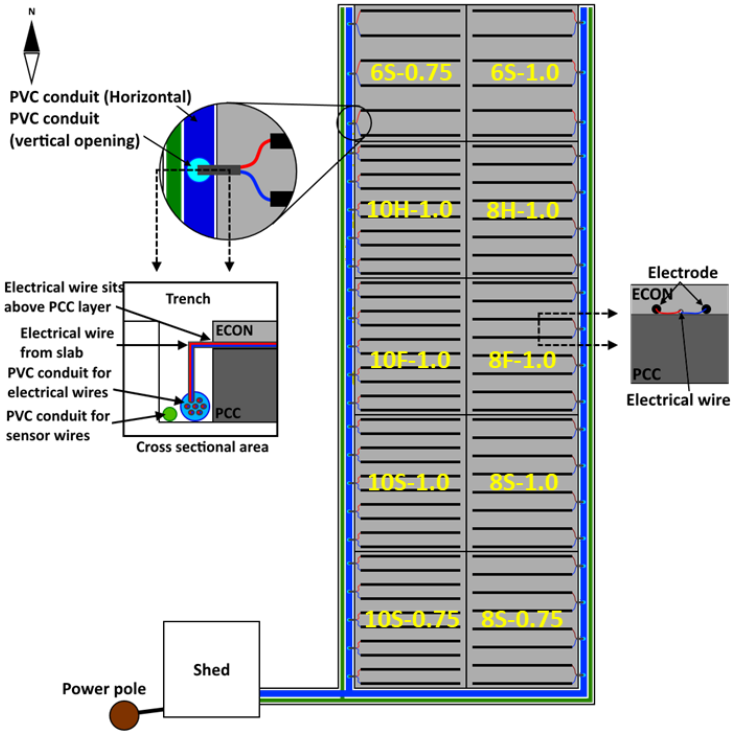

(b)

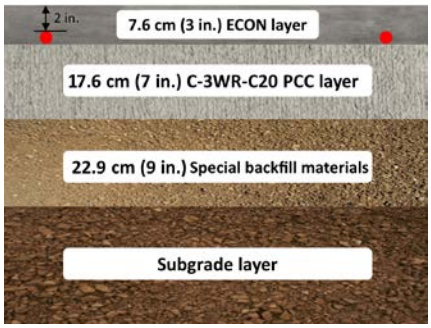

(c)

Figure 1 ECON HPS construction location and design plans: (a) construction location, (b) plan view, and (c) cross-section view.

The 10 constructed ECON slabs each have different electrode configurations. This was designed to monitor the performance of different electrode configurations in a real pavement and environmental conditions. The electrode configuration for each test section is tabulated in Table 1. Circular solid bar [1.9 cm (0.75 in.) or 2.5 cm (1.0 in.)], circular hollow bar [2.5 cm (1 in.) OD with 0.3 cm (1/8 in.) wall thickness], and flat bar [2.5 cm (1 in.) × 0.4 cm (3/16 in.)] were chosen for field implementation based on laboratory investigations conducted before the construction (*21*). Four slabs were designed with ten electrodes [50.8 cm (20.0 in.) spacing], four slabs with eight electrodes [64.8 cm (25.5 in.) spacing] and two slabs with six electrodes [91.4 cm (36.0 in.) spacing].

Each test section was given a section ID where the first number represents the number of electrodes in the test section (6, 8, or 10), following by a letter representing the type of electrode (S, H, or F), and it ends with a number indicating the size of the electrode in inches that has been used (0.75 or 1.0). As an example, a slab with an ID number of 10S-0.75 has 10 smooth circular bars with 1.9 cm (0.75 in.) outer diameter. The location of each constructed slab can be seen in Figure 1 (b).

Table 1 Electrode configuration in each slab.

Test section	Section ID	No. of electrodes (spacing)	Size of electrodes, cm (in.)	Electrode type & shape
Test section 1	10S-0.75	10 (50.8 cm/20.0 in.)	1.9 (0.75)	Smooth circular bar
Test section 2	10S-1.0	10 (50.8 cm/20.0 in.)	2.5 (1.00)	Smooth circular bar
Test section 3	10F-1.0	10 (50.8 cm/20.0 in.)	2.5 (1.00)	Flat bar
Test section 4	10H-1.0	10 (50.8 cm/20.0 in.)	2.5 (1.00)	Hollow circular bar
Test section 5	6S-0.75	8 (64.8 cm/25.5 in.)	1.9 (0.75)	Smooth circular bar
Test section 6	8S-0.75	8 (64.8 cm/25.5 in.)	1.9 (0.75)	Smooth circular bar
Test section 7	8S-1.0	8 (64.8 cm/25.5 in.)	2.5 (1.00)	Smooth circular bar
Test section 8	8F-1.0	8 (64.8 cm/25.5 in.)	2.5 (1.00)	Flat bar
Test section 9	8H-1.0	6 (91.4 cm/36.0 in.)	2.5 (1.00)	Hollow circular bar
Test section 10	6S-1.0	6 (91.4 cm/36.0 in.)	2.5 (1.00)	Smooth circular bar

3. DESCRIPTION OF MATERIALS

3.1 ECON and PCC layer Mix Design

The ECON mix design was developed based on numerous trial batches in the lab (*21*) and prior full-scale demonstration experience at DSM International Airport in 2016 (*22*). First, the research team obtained samples from aggregate, cement, fly ash, and all the admixtures from the concrete plant. Second, numerous trial batches were made in the lab in order to attain a balanced ECON mix design to meet workability and mechanical property requirements in accordance to Iowa DOT specifications as well as ensuring good electrical conductivity. Third, the concrete supplier was asked to batch three cubic yards of the ECON mix design from the laboratory phase for laboratory testing. This step was taken as a precaution step before construction to ensure that the mixture from the batch plant was consistent with the construction specifications. It was found in the trial batch that the ECON was highly workable, but on the other hand, its electrical

resistivity was high. Therefore, adjustments were made to the carbon fiber content and the admixture dosages to reduce the workability and resistivity. It was also found during the laboratory phase that (1) adding carbon fibers withholding moisture reduces the fiber loss during ECON production and (2) mixing fibers with aggregate before the presence of cementitious materials helped with achieving a better, more uniform fiber dispersion. Therefore, these suggestions were incorporated into the construction phase.

The finalized ECON mix design is shown in Table 2. The mixture contained 1.25% carbon fiber by volume, and 20% fly ash replacement. The significant differences between this mixture and its predecessors (*22*) were first introducing 20% fly ash to the mix to increase workability and durability. Second, the elimination of methylcellulose fiber dispersion agent and corrosion inhibitor admixtures in order to decrease the possibility of incompatibility between the admixtures. In addition, the carbon fiber content was increased from 1 percent to 1.25 percent by volume to account for any potential carbon fiber losses that may take place during batching and placing. The regular PCC layer (bottom layer) mix design was C-3WR-C20, and it is composed of 45% fine and 55% coarse aggregate with 20% type C fly ash. It is worth mentioning that the typical electrical resistivity of a regular concrete is about 9×10^5 Ω-cm (*23–26*), while achieved electrical resistivity for ECON was 1300 Ω-cm due to the addition of 1.25% carbon fiber into the mixture.

Table 2 ECON mix proportions for field implementation.

Components		Type	Content Kg/m^3 (lb./yd^3)
Basic	Coarse aggregate	1.9 cm (3/4 in.) limestone	585.0 (986.1)
	Intermediate aggregate	0.9 cm (3/8 in.) chips	301.5 (508.2)
	Fine aggregate	Concrete river sand	640.3 (1,079.2)
	Cement	Holcim type I/II	375.4 (632.7)
	Fly Ash	Type C	96.4 (162.5)
	Water	Potable water	199.9 (336.9)
	Carbon fiber,	0.63 cm (0.25 in.) in length	1.25 (% Vol.)
Admixtures	Air Entrainment	EUCON AEA-92	0.9 l/m^3 (3.0 oz./cwt)
	Water Reducer	EUCON WR 91	2.3 l/m^3 (7.5 oz./cwt)

3.2 Electrodes

Electrodes in ECON HPS have the role of applying the electricity to ECON layer due to their high electrical conductivity properties. All the electrodes were chosen 316L grade stainless steel, which has promising resistance to corrosion. Therefore, the electrodes would stand degradation and cracking, which will lead to system efficiency reduction and electrode debonding from ECON. Circular and flat bar electrode geometries were chosen rather than angled electrodes, which have been used in the predecessor projects (*1*) to minimize stress concentrations and thus reduce cracking potential. In addition, the chosen electrode geometries also eliminated using fiberglass bars perpendicular to the electrodes, which have been used in other projects (*1*) to minimize the possible cracking. All the electrodes were anchored to the PCC layer to secure them and minimize their movements during the pavement construction. The wires which were used to connect the electrodes to the power supply were specially selected for 208 Volts AC (VAC), 600 A usage. The wires were also designed for use in a rough environment, such as a construction project, and had a special insulation layer.

3.3 Sensors and Data Acquisition System

Both wired and wireless sensors were utilized in the demonstration project. 130 Campbell Scientific Thermocouple (type E), 40 Geokon strain gauges, 10 wireless Monnit voltage sensors, and 10 wireless Monnit current sensors were installed. Thermocouples and strain gauges were embedded within the slabs in both the ECON and PCC layer. Voltage and current wireless sensors were installed in the power distribution box within the shed to monitor the electrical consumption of each test section.

All the sensors were tested in the lab prior to the field installation. In order to gather all the data, two Campbell Scientific CR6 data loggers and five Campbell Scientific AM16/32B Multiplexers were installed in the shed. The Monnit voltage and current sensors transmit the readings to a gateway before being transferred to a cloud-based real-time monitoring system. All other sensors were connected to a laptop in the shed which can be accessed remotely through a wireless hotspot provided in the shed. Therefore, system operation tasks including turning the slabs on/off, data collection, and real-time monitoring can be easily conducted remotely.

3.4 Control System

The research team had selected a robust control system for this project. Programmable Logic Controller (PLC) is an industrial standard control system. The PLC is a modular system comprising of a CPU unit, analog temperature input module, digital output module, and relays. In addition, the modular design will allow expansion if the research team deems necessary in the future. One embedded thermocouple sensor in the center of each slab, 1.3 cm (0.5 in.) from the pavement surface, was linked to the PLC system. This enables the control system to monitor the pavement surface temperature. Once pavement surface temperature drops below a pre-determined temperature (5°C/41°F), the control system activates the 120/208 VAC power source using the relays to generate heat within the ECON layer. The ECON system can melt ice and snow much quicker in 208 VAC compare to 120 VAC and can be used in times when the winter weather conditions are particularly harsh (e.g. snow/ice storms during a polar vortex) and the road serviceability needs to be maintained continuously under such harsh conditions.

4. INSTRUMENTATION AND INSTALLATION METHODS

The instrumentation plan for EOCN HPS consists of steps that were taken for installing electrodes, sensors, data acquisition system, and a power supply system. These steps have been developed based on extensive previous experiences during both field and laboratory experiments. Figure 2 depicts the installation procedures for different components during the construction phase.

4.1 Installation of Electrodes

The location of each stainless-steel electrode was marked on each slab, and the electrodes were fixed using steel straps, as shown in Figure 2(a). A drill was used to make the holes and secure the straps to the PCC layer. After anchoring the electrodes, all the electrodes were connected to electric wires using gauge-ring wire connectors for flat bars and hose clamps for circular bars (see Figure 2(b)).

(a)

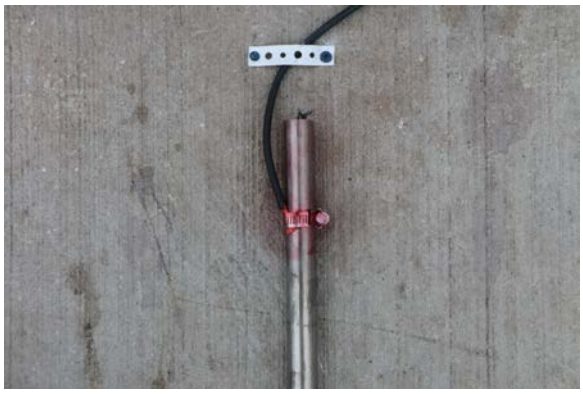

(b)

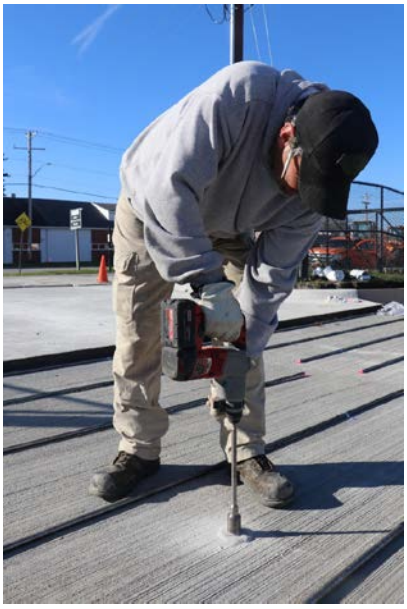

(c)

(d)

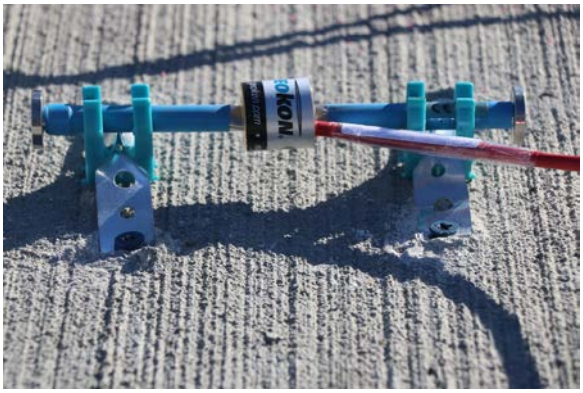

(e)

(f)

Figure 2 Electrode and sensor wiring and instrumentation: (a) anchorage of electrode to the PCC layer, (b) electrode electrical wiring, (c) thermocouple sensor tree installation, (d) thermocouple sensor placement, (e) strain gauge installation, and (f) electrical and sensor wiring in the shed.

4.2 Sensors Instrumentation Plan

Sensor instrumentation locations were chosen based on the critical response locations within a slab with regards to the temperature and strain variations. The temperature trees were mounted on a 0.6 cm (¼ in.) fiberglass bar in order to eliminate temperature and electricity gradients in different layers. A hole was first drilled in the PCC layer at the center of each slab (see Figure 2(c)), and the temperature trees were installed inside and secured with cement grout (see Figure 2(d)). Each temperature tree consisted of six thermocouples in the following locations: top and bottom of ECON layer, middle, and bottom of PCC layer, middle of the base layer, and one sensor in the subgrade layer.

Strain gauges were mounted on the PCC layer using two plastic chairs and steel straps (see Figure 2(e)). The steel straps were screwed to the PCC layer to secure them. In the case where two strain gauges needed to be placed at different depths, two 0.6 cm (¼ in.) fiberglass bars were used to place and secure the strain gauges. The chosen locations of strain gauge were center, edge, corner in wheel path direction, and corner in a diagonal direction. The strain gauges were installed both in ECON layer and PCC layer. The strain gauge configuration was chosen to measure the strain in both layers to monitor the effect of heating in the ECON layer. Sensors wires were guided to a separate PVC pipe to the shed (see Figure 2(f)). The PVC pipe for electrical wiring was not chosen to host the sensors wire to prevent possible interferences in sensor signals and for safety purposes.

4.3 Integration of Power Supply and Control System

There was no existing power supply source close to the construction site; therefore, a new 45-1 pole with 3-100kVA XFMRS was placed to the southwest corner of the site. A meter was installed on the pole to measure electrical power usage, and a power line trench was excavated from the pole to the shed. This enables powering ECON HPS test section using either a three-phase 208 VAC, or a single phase 120 VAC, both with a maximum of 600 A source. Two three-phase double pole power panels were installed in the shed with two circuit breakers. Each circuit breaker can feed five slabs with 120/208 VAC. The three-phase 208 VAC was achieved by using two lines, one for each phase, while the 120 VAC was carried in each single line. The 120 VAC was achieved using one line and the neutral. The different electrode configuration design would cause each slab to draw a different amount of current compared to the other slabs. Thus, the research team conducted a series of tests and simulations and grouped the slabs in a way to distribute the power load evenly within each phase and to eliminate overloading on one phase.

Another added feature of using PLC as a control system is electrode-based control. The electrode-based control feature gave the research team extra degree of control to create different electrode configurations (spacing) within one slab with turning on/off individual electrodes. Therefore, the research team added more relays for test sections with 10 electrodes (4 slabs) to incorporate this feature. The electrode wiring diagram for the 10 electrode slabs is shown in Figure 3(a). The other six slabs were designed using slab-based control, which can only turn all the electrodes in each slab on and off at once (Figure 3(b)). The PLC system and its wiring are being shown in Figure 3(c).

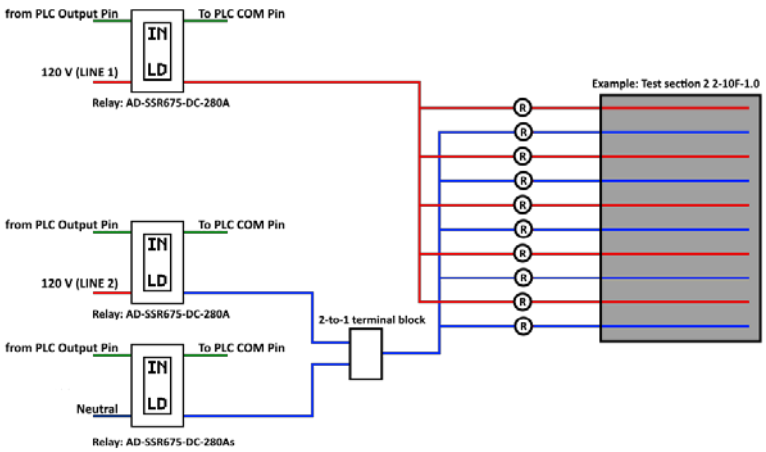

(a)

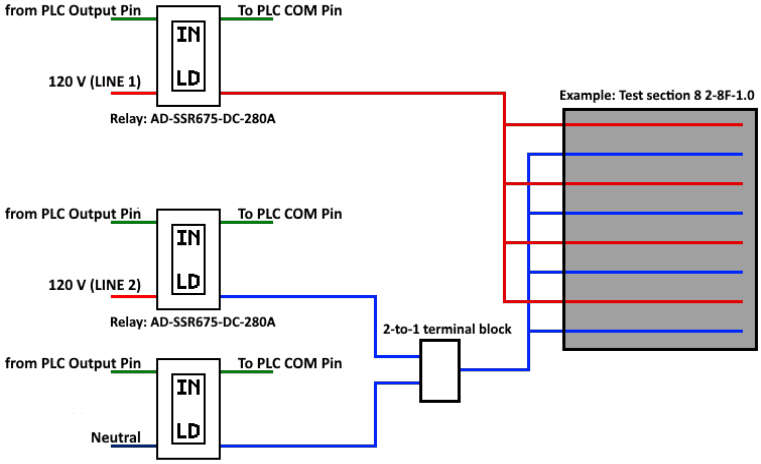

(b)

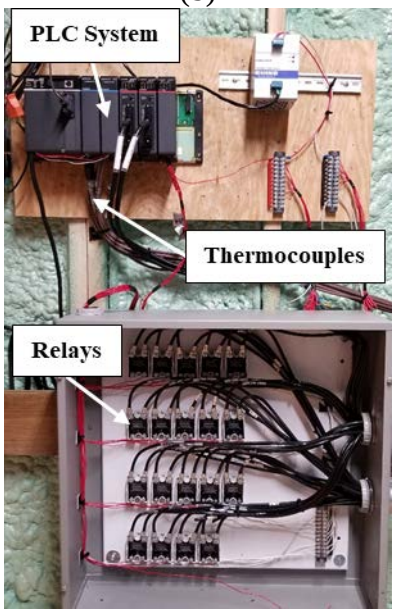

(c)

Figure 3 PLC control configurations: (a) electrode-based control (test section 1 to 4), (b) slab-based control (test section 5 to 10), (c) PLC and relay wirings.

5. CONSTRUCTION PROCEDURE

Construction started on October 11, 2018 and lasted for four weeks due to the weather condition. The existing pavement was a 40 years old PCC pavement with numerous cracks at the joints and midspan. The pavement had also been rehabilitated at several spots because of intensive damages. This parking section experiences a high amount of heavily loaded traffic, including 18-wheeler tractors and trailers, being at the entrance of the Iowa DOT receiving station. The project was a reconstruction project, and the first task was to remove the existing 15.2 cm (6 in.) concrete pavement. The existing pavement did not have any base layer, and it lacked any drainage system; therefore, a geofabric system was utilized on top of the subgrade, and a 22.9 cm (9 in.) special backfill layer was compacted for the base layer.

The ECON HPS was designed with two layers, 17.8 cm (7 in.) regular PCC layer (bottom layer) and 7.6 cm (3 in.) ECON layer (top layer). The construction steps in sequence are shown in Figure 4. Dowel bars [1.9 cm (¾ inch) in diameter] were used for proper load transfer between the adjacent slabs at sawn joints. A joint spacing of 15 feet was designed, and the joints were matched with the surrounding concrete slabs. A vibrating screed was used to compact the PCC layer (Figure 4 (a)). A broom was used perpendicular to traffic flow after finishing the PCC layer to roughen the surface and increase the bond between the bottom PCC layer and the top ECON layer (Figure 4 (b)). Curing compound was not suggested for curing the PCC layer due to its potential adverse impact on the bond between the two layers, therefore, wet curing using curing blankets was chosen for the bottom PCC layer.

The research team started mounting the electrodes on top of the PCC layer (Figure 4c). The electrodes were first washed and then dried in order to remove any debris or possible oil on their surface. This was an essential step to ensure a good bond between each electrode and the ECON layer. The perimeter of the ECON test sections, where it meets the regular concrete sections, got isolated using expansion joints to minimize any interaction and potential strain build-up with other unheated regular concrete slabs. The strain gauge and thermocouple trees were installed, and their wires were guided to its designated PVC conduits (Figure 4(d)). The surface of the PCC layer got cleaned using an air blower and damped to ensure a good bond between the two lifts (Figure 4(e)). A white flag was installed at each sensor location so that the sensors do not get stepped on during the ECON placing (Figure 4(f)).

The ECON layer was placed on October 25, 2018, and a vibrating screed was used to compact this layer (Figure 4g). In the end, the curing compound was sprayed on top of the test section (Figure 4(h)) to prevent moisture loss. The shed was placed in the southwest corner of the test section, and the wires were installed to connect the electrodes to the power supply source. Meanwhile, the joints were cut full depth through the ECON layer to match those in the bottom PCC layer. The last step in the construction phase was to fill the trenches which hold the electrical and sensor PVC conduits with 15.2 cm (6 in.) hot mix asphalt.

(a) (b) (c) (d) (e) (f) (g) (h)

Figure 4 ECON HPS construction steps: (a) C-3WR-C20 PCC placement, (b) PCC layer screeding, (c) electrode installation, (d) PVC conduit placement, (e) surface cleaning, (f) ECON layer before placement, (g) ECON placement and compaction with vibrating screed, and (h) curing compound spraying.

6. IOWA DOT ECON HPS PERFORMANCE EVALUATION

The current winter maintenance operation conducted by Iowa DOT ground crew for their parking lot consists of eight crews with eight snow removal equipment. It takes the ground crew an average of 5 hours to remove the snow from the whole Iowa DOT parking lot in a normal 5 cm (2 in.) snow event. The ground crew has been using 10 tons of deicing chemicals and sand between only January 1, 2019, and February 20, 2019. The ground crew first plow and gather the snow in several designated areas in the parking lot and then apply deicing chemicals for the remaining snow on the ground. The ground crew then haul the gathered snow from different designated locations and transfer it to the Iowa DOT south parking lot to be melt eventually by the sun. Iowa DOT sends out several emails to its employees before each snow event to move the personal and Iowa DOT owned vehicles from the parking lot to facilitate the winter snow removal operation. The deicing chemicals usually get transferred to the grass areas during the winter season, which kills the vegetation. Therefore, the ground crew needs to plant new grasses, especially near the paved area each summer season and gather all the sand which has been spread during each winter season at the beginning of spring. Nahvi et al. have done a life-cycle benefit cost analysis (LCBCA) of ECON HPS on airfield pavements and found out that the construction of ECON HPS would be 50 percent higher than the regular PCC (*27*, *28*). The current state of practice for removing ice and snow is time-consuming, labor-intensive, and environmentally unfriendly due to the usage of deicing chemicals.

Figure 5 shows the ECON HPS system performance during the period of February and March of 2019. The resistive heating performance of ECON HPS was capable of maintaining a snow and ice-free surface while the remaining parking lot was covered with about 5 cm (2 in.) of snow. A snow event started at 8 pm on February 11, 2019, and lasted until 2 am the next day (6 hours). The average air temperature and relative humidity in this period were -8.4°C (17°F) and 86%, respectively. The system started operating at 8 PM and was capable of melting all the snow by 11 pm (3 hours later) and maintaining a snow-free surface until the snow event ended.

The power density (P) is the amount of energy consumed by each slab per unit area and was calculated using the average current usage (I) and the voltage applied to the slabs during a snow event. The applied voltage for the operation was chosen 120 VAC for ECON HPS performance evaluation. The power density range for all the slabs was between 109.8 and 491.5 W/m^2 with an average of 265.1 W/m^2. There was a resistivity variation observed between the slabs, which was due to carbon fiber dispersion within each test section. Therefore, in order to compare the power demand for each electrode configuration regardless of the slab's electrical resistivity, the power density was normalized by the resistivity measurement for each slab. This normalization is necessary since the effect of resistivity is the linear inverse of power density, which means, a slab with higher resistivity has a lower power density and vice versa. This normalization is essential to only see the effect of electrode configuration and eliminate the effect of ECON resistivity on the analysis. The normalized power density for each test section and the slab surface temperature while in operation are shown in Figure 6.

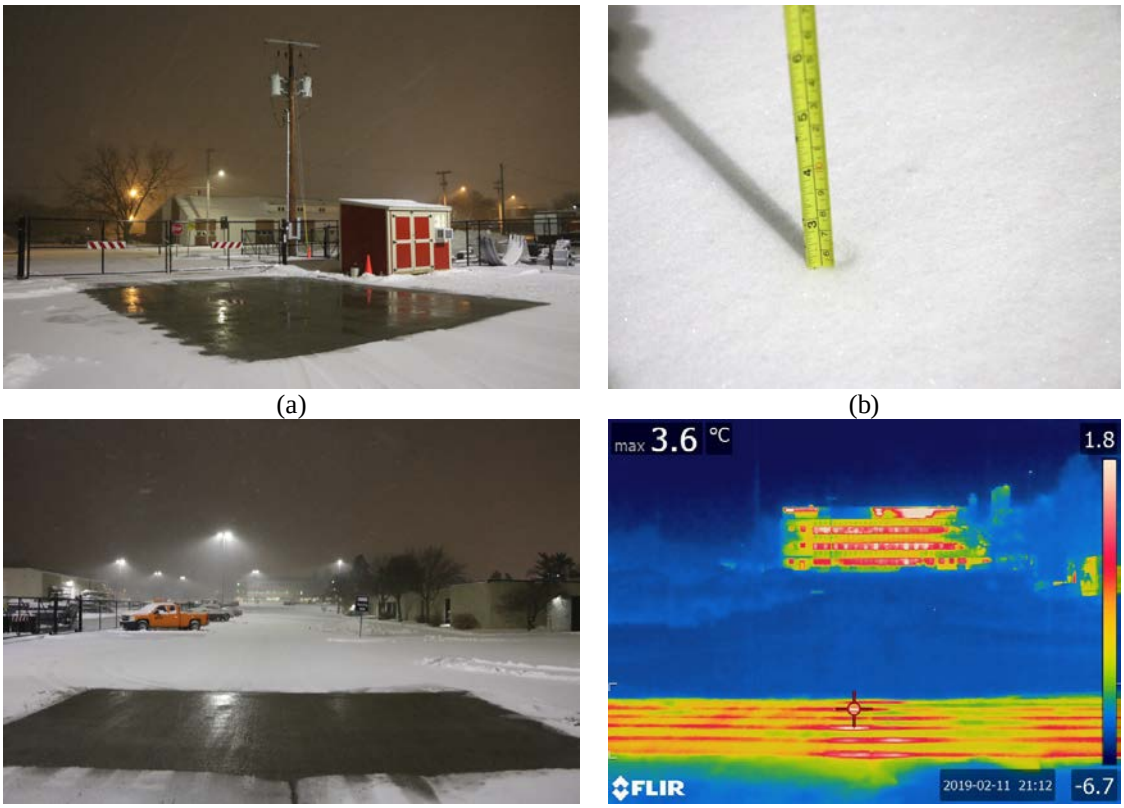

Figure 5 ECON HPS heating performance: (a) Southside slabs performance, (b) 5 cm (2 in.) of snow accumulation in the surrounding slabs, (c) Northside slabs performance, and (d) infrared thermography of ECON slabs.

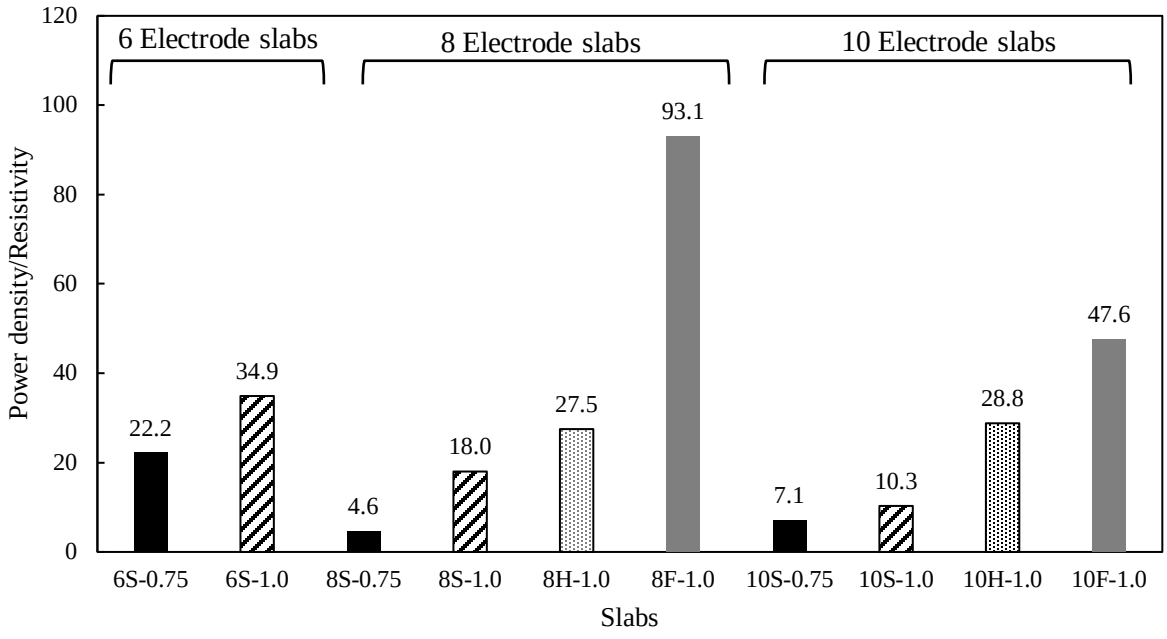

(a)

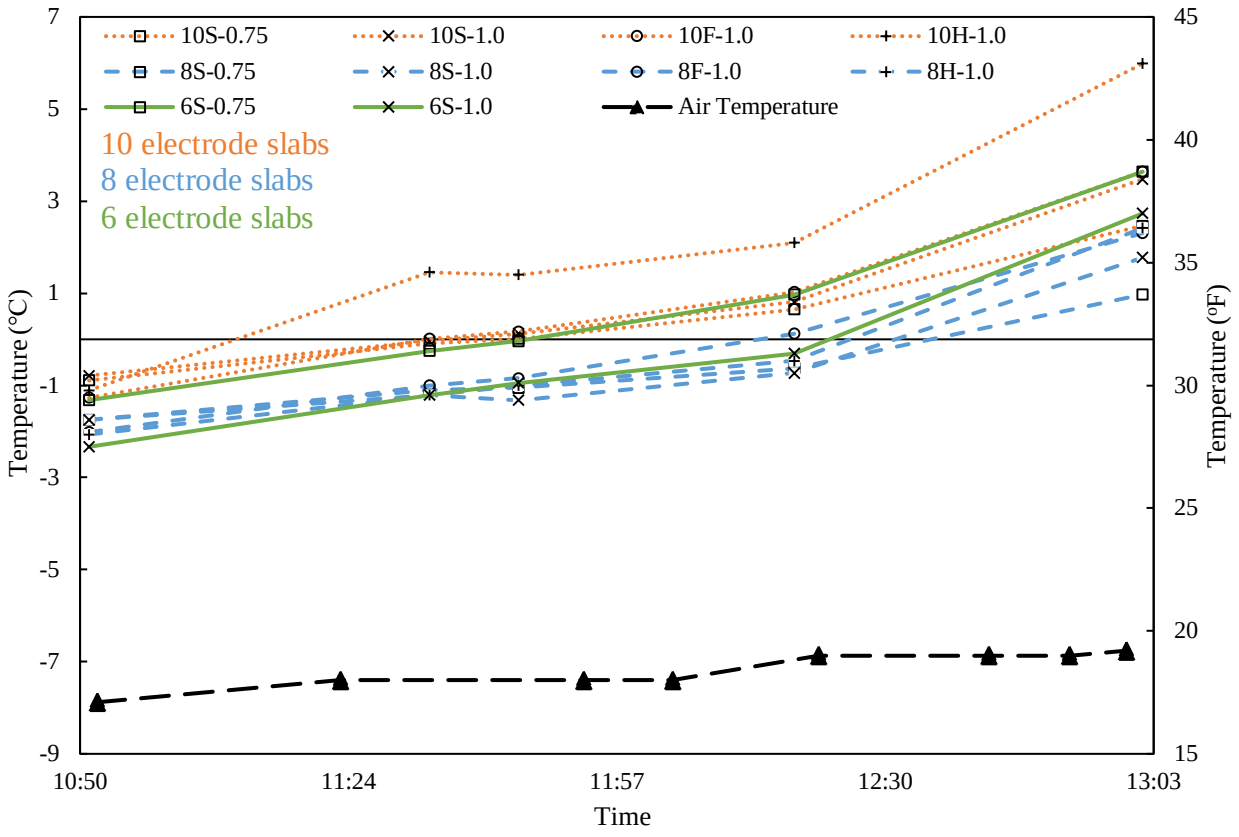

(b)

Figure 6 (a) corrected power density per square meter per resistivity of each slab, (b) slab surface temperature and air temperature vs. time

As shown in Figure 6 (a), the electrode configuration directly affects the corrected power density (power density/resistivity). In all slabs with the same number of electrodes, the slabs with flat bar (F), 2.5 cm (1 in.) hollow bar (H), 2.5 cm (1 in.) solid bar (S-1.0), and 1.9 cm (0.75 in.) solid bar (S-0.75) have the same corrected power density ranking with the flat bar having the highest and the 1.9 cm (0.75 in.) solid bar the lowest corrected power density. It has also been found that by increasing the electrode diameter in circular solid bars from 1.9 cm (0.75 in.) to 2.5 cm (1 in.), the corrected power density increased in all different spacing options, which is due to the increase in the contact area between the electrode and the ECON layer. In addition, the corrected power density decreased in flat bar and 2.5 cm (1 in.) circular solid bar by decreasing the spacing (increasing the number of electrodes within a slab).

Figure 6 (b) shows the thermal performance of each slab and the air temperature versus time. These data were gathered from the thermocouples placed 1.3 cm (0.5 in.) below the pavement surface. The temperature in each slab increased after the slab got turned on, but after some time, the slab temperature stayed constant, which is due to melting snow on the surface (phase change). 10H-1.0 slab showed the highest temperature increase (7.4°C/13.3°F in 2 hours), and the 8S-0.75 slab showed the lowest. The average temperature rise for all the slabs was 5°C (9°F) in 2 hours. The slabs with eight electrodes showed a lower heating performance compare to the slabs with 10 electrodes.

7. SUMMARY, CONCLUSIONS, AND RECOMMENDATIONS

The objective of this study was to demonstrate the design, full-scale demonstration, and performance monitoring of the largest operational electrically conductive concrete (ECON) heated pavement system (HPS). Ten ECON test slabs were designed and constructed at the south parking lot of Iowa DOT headquarter in Ames, Iowa on October of 2018. Programmable logic controller (PLC) system and slab instrumentation using temperature sensors were designed and implemented for the remote-control operation and system performance monitoring respectively. The deicing and anti-icing performance of ECON HPS was evaluated during February to March of 2019. The summarized findings of this study, along with the recommended future investigations are as follows:

- Ten ECON HPS test slabs with different electrode configurations were constructed in the south parking lot of Iowa DOT headquarter as the largest ECON HPS implementation project. All the test slabs showed promising snow and ice-free capabilities through various winter weather events.
- A PLC system was designed, programmed, and implemented in the construction and it showed a promising and robust remote-control system to be used in ECON HPS technology.
- Each ECON HPS test slab had a different electrode design configuration, including electrode shape, size, and spacing compared to other test slabs. In all different spacing options, the flat bar, 2.5 cm (1 in.) hollow bar, 2.5 cm (1 in.) solid bar, and 1.9 cm (0.75 in.) solid bar have the same power density ranking with the flat bar having the highest and the 1.9 cm (0.75 in.) solid bar the lowest power density.
- The power density range for all the slabs was between 109.8 and 491.5 W/m^2 with an average of 265.1 W/m^2. The power density normalized by the resistivity of each ECON HPS slab ranges between 4.6 W/m^2 (slab 8S-0.75) to 93.1 W/m^2 (slab 8F-1).
- Increasing the electrode diameter in circular solid bars resulted in an increase in the power density in all electrode spacing.
- The power density decreased in flat bar and 1 in. circular solid bar by decreasing the electrode spacing (increasing the number of the electrodes used in each slab).

The findings of this study facilitate the design of ECON HPS and provide detailed information on the construction steps. The ECON HPS performance will be monitored in the upcoming winter seasons, and the performance of each designed configuration will be evaluated through a thorough economic analysis. The electrical safety and other related issues that might arise during the operation will also be considered.

ACKNOWLEDGMENTS

The authors would like to thank the Iowa Department of Transportation (DOT) and the Iowa Highway Research Board (IHRB) for providing the matching funds for this research project which is sponsored by the Federal Aviation Administration (FAA). The authors would also like to thank the FAA Air Transportation Center of Excellence for the Partnership to Enhance General Aviation Safety, Accessibility and Sustainability (PEGASAS). The IHRB technical

advisory committee (TAC) members from Iowa DOT and Iowa Counties, particularly Mr. Mike Harvey, Director of Iowa DOT's Support Services Office Administrative Services Division, and Iowa DOT electricians, the FAA PEGASAS Technical Monitor for Heated Airport Pavements project, and Mr. Gary L. Mitchell of the American Concrete Pavement Association (ACPA) are gratefully acknowledged for their guidance, support, and direction throughout the research. The authors would like to express their sincere gratitude to other research team members from ISU's Program for Sustainable Pavement Engineering and Research (PROSPER) at Institute for Transportation for their assistance with the lab and field investigations. Although the Iowa DOT and FAA have sponsored this study, they neither endorse nor reject the findings of this research. The presentation of this information is in the interest of invoking comments by the technical community with respect to the results and conclusions of the research. This paper does not constitute a standard, specification, or regulation.

AUTHOR CONTRIBUTION STATEMENT

The authors confirm contribution to the paper as follows: study conception and design: Dr. Halil Ceylan, Dr. Sunghwan Kim, Dr. Mani Mina, Dr. Kristen Cetin, Dr. Peter C. Taylor, Amir Malakooti, Wei Shen Theh, and Sajed Sadati; data collection: Amir Malakooti, Wei Shen Theh, and Sajed Sadati; analysis and interpretation of results: Amir Malakooti, Wei Shen Theh, Sajed Sadati, Dr. Halil Ceylan, and Dr. Sunghwan Kim: draft manuscript preparation: Amir Malakooti, Wei Shen Theh, Sajed Sadati, Dr. Halil Ceylan, Dr. Sunghwan Kim, Dr. Kristen Cetin and Dr. Peter C. Taylor. All authors reviewed the results and approved the final version of the manuscript.

REFERENCES

1. Abdualla, H., H. Ceylan, S. Kim, M. Mina, K. S. Cetin, P. C. Taylor, K. Gopalakrishnan, B. Cetin, S. Yang, and A. Vidyadharan. Design and Construction of the World's First Full-Scale Electrically Conductive Concrete Heated Airport Pavement System at a U.S. Airport. *Transportation Research Record*, No. November, 2018. https://doi.org/10.1177/0361198118791624.
2. Sadati, S. M. S., K. Cetin, H. Ceylan, A. Sassani, and S. Kim. Energy and Thermal Performance Evaluation of an Automated Snow and Ice Removal System at Airports Using Numerical Modeling and Field Measurements. *Sustainable Cities and Society*, Vol. 43, No. August, 2018, pp. 238–250. https://doi.org/10.1016/j.scs.2018.08.021.
3. Tuan, C. Y. *Concrete Technology Today: Conductive Concrete for Bridge Deck Deicing*. Nebraska Department of Roads, 2004.
4. Sassani, A., H. Ceylan, S. Kim, K. Gopalakrishnan, A. Arabzadeh, and P. C. Taylor. Influence of Mix Design Variables on Engineering Properties of Carbon Fiber-Modified Electrically Conductive Concrete. *Construction and Building Materials*, Vol. 152, 2017, pp. 168–181. https://doi.org/10.1016/j.conbuildmat.2017.06.172.
5. Pan, P., S. Wu, Y. Xiao, and G. Liu. A Review on Hydronic Asphalt Pavement for Energy Harvesting and Snow Melting. *Renewable and Sustainable Energy Reviews*, Vol. 48, 2015, pp. 624–634. https://doi.org/10.1016/j.rser.2015.04.029.
6. Pan, P., S. Wu, F. Xiao, L. Pang, and Y. Xiao. Conductive Asphalt Concrete: A Review on Structure Design, Performance, and Practical Applications. *Journal of Intelligent Material Systems and Structures*, Vol. 26, No. 7, 2014, pp. 755–769. https://doi.org/10.1177/1045389X14530594.
7. Ceylan, H., K. Gopalakrishnan, S. Kim, and W. Cord. Heated Transportation Infrastructure Systems: Existing and Emerging Technologies. *12th International Symposium on Concrete Roads*, 2014.
8. Arabzadeh, A., H. Ceylan, S. Kim, K. Gopalakrishnan, A. Sassani, S. Sundararajan, and P. C. Taylor. Superhydrophobic Coatings on Portland Cement Concrete Surfaces. *Construction and Building Materials*, Vol. 141, 2017, pp. 393–401. https://doi.org/10.1016/J.CONBUILDMAT.2017.03.012.
9. Gopalakrishnan, K., H. Ceylan, S. Kim, S. Yang, and H. Abdualla. Electrically Conductive Mortar Characterization for Self-Heating Airfield Concrete Pavement Mix Design. *International Journal of Pavement Research and Technology*, Vol. 8, No. 5, 2015, pp. 315–324.
10. Arabzadeh, A., A. Sassani, H. Ceylan, S. Kim, K. Gopalakrishnan, and P. C. Taylor. Comparison between Cement Paste and Asphalt Mastic Modified by Carbonaceous Materials: Electrical and Thermal Properties. *Construction and Building Materials*, Vol. 213, 2019, pp. 121–130. https://doi.org/10.1016/j.conbuildmat.2019.04.060.
11. Notani, M. A., A. Arabzadeh, H. Ceylan, S. Kim, and K. Gopalakrishnan. Effect of Carbon-Fiber Properties on Volumetrics and Ohmic Heating of Electrically Conductive Asphalt Concrete. *Journal of Materials in Civil Engineering*, Vol. 31, No. 9, 2019, p. 04019200. https://doi.org/10.1061/(ASCE)MT.1943-5533.0002868.
12. Sassani, A., A. Arabzadeh, H. Ceylan, S. Kim, S. M. S. Sadati, K. Gopalakrishnan, P. C. Taylor, and H. Abdualla. Carbon Fiber-Based Electrically Conductive Concrete for Salt-Free Deicing of Pavements. *Journal of Cleaner Production*, Vol. 203, 2018, pp. 799–809.

https://doi.org/10.1016/j.jclepro.2018.08.315.
13. FAA. Voluntary Airport Low Emissions Program (VALE). https://www.faa.gov/airports/environmental/vale/.
14. Kilkiş, B., and Ş. Kilkiş. New Exergy Metrics for Energy, Environment, and Economy Nexus and Optimum Design Model for Nearly-Zero Exergy Airport (NZEXAP) Systems. *Energy*, Vol. 140, 2016, pp. 1–21. https://doi.org/10.1016/j.energy.2017.04.129.
15. Abdualla, H., H. Ceylan, K. S. Cetin, S. Kim, P. C. Taylor, M. Mina, B. Cetin, K. Gopalakrishnan, and S. Sadati. Construction Techniques for Electrically Conductive Heated Pavement Systems.
16. Abdualla, H. *Design, Construction, and Performance of Heated Concrete Pavements System*. Iowa State University, Digital Repository, Ames, 2018.
17. Sadati, S. S., K. Cetin, Ceylan, and Halil. Numerical Modeling of Electrically Conductive Pavement Systems. *Congress on Technical Advancement*, 2017, pp. 111–120.
18. Sadati, S. M. S., K. S. Cetin, H. Ceylan, and S. Kim. *A Methodology for Investigating Different Electrode Design Configurations of Electrically Conductive Concrete Heated Pavement Systems*. 2019.
19. Alimohammadi, H., and B. Izadi Babokani. Finite Element Analysis of a Piezoelectric Layered Plate with Different Materials. *International Journal of Engineering and Applied Sciences (IJEAS)*, Vol. 6, No. 8, 2019, pp. 18–21.
20. *Iowa Department of Transportation Standard Specification with GS-15008 Revisions*.
21. Malakooti, A., H. Abdualla, A. Sassani, H. Ceylan, and S. Kim. Effect of Electrode Geometry and Size on Heating Performance of Electrically Conductive Concrete (19-02535). 2019.
22. Sassani, A., H. Ceylan, S. Kim, A. Arabzadeh, P. C. Taylor, and K. Gopalakrishnan. Development of Carbon Fiber-Modified Electrically Conductive Concrete for Implementation in Des Moines International Airport. *Case Studies in Construction Materials*, Vol. 8, 2018, pp. 277–291. https://doi.org/10.1016/j.cscm.2018.02.003.
23. Malakooti, A. *Investigation of Concrete Electrical Resistivity As a Performance Based Test*. Utah State University, 2017.
24. Melugiri-Shankaramurthy, B., Y. Sargam, X. Zhang, W. Sun, K. Wang, and H. Qin. Evaluation of Cement Paste Containing Recycled Stainless Steel Powder for Sustainable Additive Manufacturing. *Construction and Building Materials*, Vol. 227, 2019, p. 116696. https://doi.org/10.1016/j.conbuildmat.2019.116696.
25. Malakooti, A., M. Maguire, and R. J. Thomas. Evaluating Electrical Resistivity as a Performance Based Test for Utah Bridge Deck Concrete (CAIT-UTC-NC35). *Rutgers University. Center for Advanced Infrastructure and Transportation*, 2018.
26. Mosavi, H., R. Alrashidi, M. Almarshoud, M. H. Alyami, K. A. Riding, C. C. Ferraro, M. D. A. Thomas, and H. DeFord. Use of Electrical Test Method on Determination Aging Factor of Concrete Incorporating Supplementary Cementitious Materials. In *RILEM Bookseries*, Springer Netherlands, pp. 299–306.
27. Habibzadeh-Bigdarvish, O., X. Yu, G. Lei, T. Li, and A. J. Puppala. Life-Cycle Cost-Benefit Analysis of Bridge Deck de-Icing Using Geothermal Heat Pump System: A Case Study of North Texas. *Sustainable Cities and Society*, Vol. 47, 2019, p. 101492. https://doi.org/10.1016/j.scs.2019.101492.
28. Nahvi, A., S. M. S. Sadati, K. Cetin, H. Ceylan, A. Sassani, and S. Kim. Towards Resilient Infrastructure Systems for Winter Weather Events: Integrated Stochastic

Economic Evaluation of Electrically Conductive Heated Airfield Pavements. *Sustainable Cities and Society*, Vol. 41, No. June, 2018, pp. 195–204. https://doi.org/10.1016/j.scs.2018.05.014.